Inorg. Chem. **2002**, *41*, 1728–1738

Two-Electron Transfer for $Tl(aq)^{3+}/Tl(aq)^{+}$ Revisited. Common Virtual $[Tl^{II}-Tl^{II}]^{4+}$ Intermediate for Homogeneous (Superexchange) and Electrode (Sequential) Mechanisms

Dimitri E. Khoshtariya*[,†,‡] and Tina D. Dolidze[†]

Institute of Inorganic Chemistry and Electrochemistry, Jikiya 7, Tbilisi 380086, and Institute of Molecular Biology and Biophysics, Gotua 14, Tbilisi 380060, Georgian Academy of Sciences, Georgian Republic

Leonid D. Zusman[§]

Department of Chemistry, University of Pittsburgh, Pittsburgh, Pennsylvania 15260, and Institute of Inorganic Chemistry, Russian Academy of Sciences, Novosibirsk 630090, Russia

Göran Lindbergh[||] and Julius Glaser*[,⊥]

Department of Applied Electrochemistry and Department of Inorganic Chemistry, Royal Institute of Technology (KTH), S-100 44 Stockholm, Sweden

Received January 15, 2001

Homogeneous and electrochemical two-electron transfers within the $Tl(aq)^{3+}/Tl(aq)^{+}$ couple are considered on a common conceptual basis. For the 2 equiv electrochemical reduction of $Tl(aq)^{3+}$ to $Tl(aq)^{+}$, the intermediate state with a formal reduction potential, $E_1^* = 1.04 \pm 0.10$ V vs the normal hydrogen electrode, was detected, different from the established value of 0.33 V for a Tl^{3+}/Tl^{2+} couple. Examination of obtained electrochemical (cyclic voltammetry (CV) and rotating disk electrode techniques, along with the CV-curve computer simulation procedure) and literature data indicate that the detected formal potential cannot be the property of electrode-adsorbed species, but rather of the covalently interacting dithallium intermediate $[Tl^{II}–Tl^{II}]^{4+}$ located at the outer Helmholtz plane. The analysis of microscopic mechanisms, based on the recent hypothesis of H. Taube and the Marcus–Hush theory extended by Zusman and Beratan, and Koper and Schmickler, revealed that the homogeneous process most probably takes place through the superexchange inner-sphere two-electron-transfer mechanism, via an essentially virtual (undetectable) dithallium intermediate. In contrast, the electrochemical process occurs through a sequential mechanism, via the rate-determining step of $Tl(aq)^{2+}$ ion formation immediately followed by activationless formation of the metastable (CV-active) dithallium state. The second electrochemical electron-transfer step is fast, and shows up only in the peak height (but not in the shape) of the observed CV cathodic wave. The anodic wave for a microscopically reverse process of the oxidation of $Tl(aq)^{+}$ to $Tl(aq)^{3+}$ cannot be observed within the considered potential range due to the blocking of through-space electron transfer by the competitor process of ion transfer to the electrode.

Introduction

Microscopic mechanisms of two kinds of internally linked, homogeneous and electrochemical, two-electron-transfer processes, as well as interrelations between them, is a long-standing but still unsettled field of modern charge-transfer chemistry.[1–4] In particular, two-electron self-exchange reaction between the $Tl(aq)^{3+}$ and $Tl(aq)^{+}$ ions in aqueous solutions has been intensively studied, and is assumed now

* To whom correspondence should be addressed. E-mail: (D.E.K.) Dimitri.k@joker.ge. (J.G.) Julius@inorg.kth.se.
† Institute of Inorganic Chemistry and Electrochemistry.
‡ Institute of Molecular Biology and Biophysics.
§ Deceased.
|| Department of Applied Electrochemistry.
⊥ Department of Inorganic Chemistry.

(1) (a) Cannon R. D. *Electron-Transfer Reactions*; Butterworth: London, 1980; Chapter 2. (b) Lappin, A. G. *Redox Mechanisms in Inorganic Chemistry*; Horwood: New York, 1994.
(2) (a) Zusman, L. D.; Beratan, D. N. *J. Chem. Phys.* **1996**, *105*, 165. (b) *J. Phys. Chem. A* **1997**, *101*, 4136.

10.1021/ic0100525 CCC: $22.00
Published on Web 03/12/2002

to be the best-understood homogeneous two-electron-transfer reaction.[4−6] In all studied cases, the reaction has been found to be first-order with respect to both $[Tl^{3+}]$ and $[Tl^{+}]$,[1a,4a,b,5] which is compatible with simultaneous 2 equiv charge transfer, eq 1, but also with the stepwise mechanism via the formation of two Tl^{2+} ions (or their associates) in the intermediate state, eq 2.

$$Tl^{3+} + Tl^{+} \leftrightarrow Tl^{+} + Tl^{3+} \quad (1)$$

$$Tl^{3+} + Tl^{+} \leftrightarrow 2Tl^{2+} \leftrightarrow Tl^{+} + Tl^{3+} \quad (2)$$

For the homogeneous overall two-electron self-exchange process involving the $Tl(aq)^{+}/Tl(aq)^{3+}$ redox couple the simultaneous 2 equiv outer-sphere charge-transfer mechanism was advocated because all tests for thallium(II) in the reacting system have proved negative.[1a,4b,5,6] Participation of $Tl(aq)^{2+}$ as an intermediate has also been excluded on energy grounds by invoking the following standard reduction potentials:[4b,6,7]

$$Tl^{3+} + e^{-} \leftrightarrow Tl^{2+} \qquad E_1^{\circ} = 0.33 \pm 0.05 \text{ V} \quad (3)$$

$$Tl^{2+} + e^{-} \leftrightarrow Tl^{+} \qquad E_2^{\circ} = 2.22 \pm 0.05 \text{ V} \quad (4)$$

(All potentials are given vs the normal hydrogen electrode (NHE) as a reference.) The standard reduction potential for the overall reaction[7] is

$$Tl^{3+} + 2e^{-} \leftrightarrow Tl^{+} \qquad E^{\circ} = 1.25 \pm 0.02 \text{ V} \quad (5)$$

The free energy gap of 43 kcal mol^{-1}, calculated for such an intermediate state (eq 2) on the basis of eqs 3 and 4, is incompatible with the experimental activation free energy of the process, 23.6 kcal mol^{-1} (vide infra). However, serious restrictions exist also for a simultaneous outer-sphere two-electron-transfer mechanism emerging from major parameters of the charge-transfer theory (see the Discussion).[2,8] Yet, various authors adopt different mechanisms.[1,4−6,9−11] For the homogeneous 2 equiv self-exchange between $Tl(aq)^{3+}$ and $Tl(aq)^{+}$ ions, Hush estimated in his pioneering work the actual (acting) standard reduction potentials for 1 equiv redox steps (eqs 3 and 4) to be 1.0 and 1.5 V, respectively, on the basis of the experimental kinetic data and reasonable thermodynamic assumptions (vide infra).[10a] These values suggest a free energy gap of ca. 10−12 kcal mol^{-1} for a dismutation/disproportionation process

$$Tl^{3+} + Tl^{+} \leftrightarrow 2Tl^{2+} \quad (6)$$

(proposed by Hush as the component steps for the sequential two-electron self-exchange), and differ dramatically from the values of 0.33 and 2.22 V, respectively (eqs 3 and 4), obtained later on the basis of experiments with $Tl(aq)^{2+}$ generated directly by flash photolysis, or pulse radiolysis of thallium(III) solutions,[6] and verified for a wide class of redox cross-reactions.[1a,18] In addition, a mechanism involving a directly metal−metal bonded intermediate state, $[Tl^{II}-Tl^{II}]^{4+}$, was suggested recently by H. Taube (cf. ref 4b). Except for this suggestion, neither of the earlier authors took into account the formation of a direct $Tl^{II}-Tl^{II}$ covalent interaction as a possible reason for the lowering of the free energy of the intermediate state for a two-step two-electron self-exchange process, via the following mechanism:

$$[Tl^{III}]^{3+} + [Tl^{I}]^{+} \leftrightarrow [Tl^{II}-Tl^{II}]^{4+} \quad (7)$$

$$[Tl^{II}-Tl^{II}]^{4+} \leftrightarrow [Tl^{I}]^{+} + [Tl^{III}]^{3+} \quad (8)$$

It should be noted here that *all the previous calculations of the redox potentials (eqs 3 and 4) and the equilibrium constants for the dismutation/disproportionation process (eq 6) were derived mostly from indirect kinetic studies[6,18] performed under experimental conditions where the covalently bonded dithallium complex could not be formed or observed due to the diffusion limitations*. More recently, covalent interaction between two Tl^{2+} ions has been observed in the crystal structure of the novel $Tl^{II}_{0.8}Sn_{0.6}Mo_7O_{11}$ clusters,[15a] and the compound tetrakis(hypersilyl)dithallium(II),[15b] revealing a thallium(II)−thallium(II) covalent separation of 2.8−2.9 Å (which is ca. 0.2 Å less than twice the value of the covalent radius of the element). Structural and quantum-chemical data exist also for the stable isoelectronic dimers $Au^{0}-Au^{0}$ [16a] and $Hg^{I}-Hg^{I}$ [16b] (vide infra). Moreover, the water-soluble dimercury cation $[(aq)Hg^{I}-Hg^{I}(aq)]^{2+}$ has been

(3) (a) Koper, M. T. M.; Schmickler, W. *J. Electroanal. Chem.* **1998**, *450*, 83. (b) Boroda, Y. G.; Voth, G. A. *J. Electroanal. Chem.* **1998**, *450*, 95.

(4) (a) Lee, A. G. *The Chemistry of Thallium*; Elsevier: Amsterdam, 1971; Chapter 9. (b) Glaser, J. *Adv. Inorg. Chem.* **1995**, *43*, and references therein. (c) Cotton, F. A.; Wilkinson, G. *Advanced Inorganic Chemistry*; Interscience Publishers: New York, 1967; Chapter 18. (d) Blixt, J.; Glaser, J.; Mink, J.; Persson, I.; Persson, P.; Sandström, M. *J. Am. Chem. Soc.* **1995**, *117*, 5089−5104.

(5) (a) Roig, E.; Dodson R. W. *J. Phys. Chem.* **1961**, *65*, 2195. (b) Sykes, A. G. *Adv. Inorg. Chem. Radiochem.* **1967**, *10*, 153.

(6) (a) Falcinella, B.; Felgate, P. D.; Laurence, G. S. *J. Chem. Soc., Dalton Trans.* **1974**, 1367. (b) Schwarz, H. A.; Comstock, D.; Yandell, J. K.; Dodson, R. W. *J. Phys. Chem.* **1974**, *78*, 488.

(7) Bellavance, M. I.; Miller, B. In *Encyclopedia of Electrochemistry of the Elements*; Bard, A. J., Ed.; Marcell Dekker: New York, 1975; Vol. IV, Chapter 4.

(8) (a) Gurnee, E. F.; Magee, J. L. *J. Chem. Phys.* **1957**, *26*, 1237. (b) Taube H. *Adv. Inorg. Chem. Radiochem.* **1959**, *1*, 1.

(9) (a) Prestwood, R. J.; Wahl, A. C. *J. Am. Chem. Soc.* **1949**, *71*, 3137. (b) Harbottle G.; Dodson, R. W. *J. Am. Chem. Soc.* **1951**, *73*, 2442.

(10) (a) Hush, N. *Trans. Faraday Soc.* **1961**, *57*, 557. (b) Hush's semiphenomenological model was based on the experimental kinetic data and reasonable thermodynamic assumptions. Hence, the subsequent estimates gave actual operating values for E_1° and E_2° without any specification of the nature of the intermediate state (specified further in the present work).

(11) (a) Adamson, M. G.; Stranks, D. R. *Chem. Commun.* **1967**, 648. (b) Stranks, D. R.; Yandell, J. K. *J. Phys. Chem.* **1969**, *73*, 840.

(12) (a) Vetter, K. J.; Thiemke, G. *Z. Elektrochem.* **1960**, *64*, 805. (b) Vetter, K. J. *Elektrochemische Kinetik*; Springer: Berlin, 1961; Chapter 4.

(13) (a) Jordan, J.; Caterino, H. A. *J. Phys. Chem.* **1963**, *67*, 2241. (b) Caterino, H. A.; Jordan, J. *Talanta* **1964**, *11*, 159.

(14) (a) Ulstrup, J. *Electrochim. Acta* **1968**, *13*, 535. (b) James, S. D. *Electrochim. Acta* **1967**, *12*, 939.

(15) (a) Dronskowski, R.; Simon, A. *Angew. Chem., Int. Ed. Engl.* **1989**, *28*, 758. (b) Henkel, S.; Klenkhammer, K. W.; Schwarz, W. *Angew. Chem., Int. Ed. Engl.* **1994**, *33*, 681.

(16) (a) Ermler, W. C.; Lee, Y. S.; Pitzer, K. S. *J. Chem. Phys.* **1979**, *70*, 293. (b) Kleier D. A.; Wadt W. R. *J. Am. Chem. Soc.* **1980**, *102*, 6909. (c) Mason W. R. *Inorg. Chem.* **1983**, *22*, 147.

(17) (a) Zusman, L. D.; Beratan, D. N. *J. Chem. Phys.* **1999**, *110*, 10468. (b) Zusman, L. D. Unpublished results.

(18) (a) Falcinella, B.; Felgate, P. D.; Laurence, G. S. *J. Chem. Soc., Dalton Trans.* **1975**, 1. (b) Dodson, R. W.; Schwarz, H. A. *J. Phys. Chem.* **1974**, *78*, 892.

identified in the liquid phase as a thermodynamically stable binuclear compound.[16c] Hence, the extent of available kinetic and structural data for homogeneous systems does not exclude, but rather favors, the inner-sphere mechanism via the directly covalently bonded intermediate $[Tl^{II}-Tl^{II}]^{4+}$. However, a large and negative volume of activation, $\Delta V_a = -13.2(\pm 1.0)$ cm^3 mol^{-1}, found experimentally for this two-electron exchange process,[4a,11a] was interpreted as excluding the inner-sphere mechanism thought to require the expulsion of at least one aqua ligand in the transition state (dissociative path regarding the ligand performance), leading to a positive volume of activation.[19] This interpretation is probably not correct: the $Tl(aq)^+$ ion is only very weakly solvated,[4b] and the solvation is significantly strengthened with increasing charge on the metal ion, eventually leading to a firm, octahedral six-coordination for $Tl(aq)^{3+}$,[4b,d] which would rather lead to an associative path and, as a result, to a negative activation volume for the electron-transfer process.

Some electrochemical accounts are also available in the literature,[12−14] usually discussed separately from the homogeneous data. The most reliable (though limited) data were obtained for the reduction of $Tl(aq)^{3+}$ to $Tl(aq)^+$, while data for the oxidation of $Tl(aq)^+$ are scarce and rather dubious. The earlier electrochemical studies were performed by means of steady-state techniques only, despite the fact that the cyclic voltammetry technique, one of the most powerful techniques for the analysis of reaction mechanisms, was designed already in the mid-1960s.[26] The striking points not addressed in previous work are how the standard reduction potentials of the individual steps of the overall 2 equiv process, determined from the homogeneous solution experiments, may show up in electrochemical studies, and how the homogeneous and electrochemical two-electron-transfer processes are related to each other. In summary, the current situation for understanding the microscopic mechanisms for both processes, homogeneous and electrochemical, within the Tl^I/Tl^{III} redox couple remains contradictory and far from a satisfactory qualitative and quantitative comprehension. In the present paper, invoking the basis of new electrochemical data along with the published structural data for Tl^{II}-containing and related isoelectronic two-center systems[15,16] and on the basis of recent theoretical developments,[2,3,17] we present mutually consistent and self-consistent models for both homogeneous and electrochemical two-electron-transfer processes involving the $Tl(aq)^{3+}/Tl(aq)^+$ couple with the implication of the virtual covalently interacting intermediate $[Tl^{II}-Tl^{II}]^{4+}$.

Experimental Section

The electrochemical (cyclic voltammetry (CV) and rotating disk electrode (RDE)) experiments were carried out on a PAR 273 (Princeton Instruments) potentiostat/galvanostat, controlled by EG&G model software. Two kinds of cells with standard three-electrode configurations (Princeton), containing 50 and 5 mL of working solution, were applied. Glassy carbon working electrodes (areas 0.1256 and 0.0314 cm^2, respectively) were cleaned before each series of experiments by polishing with 1.0, 0.3, and 0.05 μm granulosites of alumina from Buehler on a Buehler polishing cloth, followed by sonification in purified water. Metal electrodes (Pt, Au) were not used to avoid complications due to the limited reproducibility and significant hysteresis of the current/voltage curves (probably caused by formation of oxide films) observed earlier.[14] More sound results for the Pt electrode were obtained by Vetter and Thiemke[12] using 7.5 M H_2SO_4 as a supporting electrolyte under conditions at which, however, the intrinsic mechanism of the electrode process itself might have been affected through the active site potential near the electrode[12] (vide infra). A saturated calomel reference electrode and a silver/silver reference chloride electrode were used as reference electrodes. They were separated from the main cell compartment by a Luggin capillary or by a glass frit. These configurations minimize contamination of working solutions by chloride ions present in reference electrode compartments. The data obtained were independent of time (within a few hours) and the cell (reference electrode) configuration, thus excluding the complexation effects between Tl^{3+} and Cl^-. All potentials quoted in this paper are referred to an NHE scale. All measurements were performed at room temperature, 24 ± 1 °C.

Working solutions were prepared from the stock solution of Tl^{III} containing 1.02 M $Tl^{III}(ClO_4)_3$ + 7.28 M $HClO_4$ and Tl^I as an impurity (≤1%), by dissolving it in appropriate aqueous solutions of $HClO_4$ and/or $NaClO_4$. The processing of the stock solution was described previously.[27] Ultrapure water was supplied by a Millipore Milli-Q system. All other chemicals used were commercial products of the highest purity available. Computer simulation procedures for CV data were run using the CVSIM program (see the Results and Data Analysis and Supporting Information, Figure S1).[28a] The concentration of Tl^{III} was varied between 2×10^{-3} and 2×10^{-2} M, which did not have any significant influence on the CV and RDE results.

Results and Data Analysis

At any solution composition explored, within the potential range of +2.0 to −0.4, the voltammograms exhibited only one reduction wave for the $Tl(aq)^{3+}/Tl(aq)^+$ couple. Within the potential region of −0.4 to −0.6, the reduction and oxidation waves for a $Tl(aq)^+/Tl^0$ couple were observed (known to be electrochemically reversible[7]) when $Tl(aq)^+$

(19) (a) Candlin, J. P.; Halpern, J. *Inorg. Chem.* **1965**, *6*, 1086. (b) Swaddle, T. W. *Inorg. Chem.* **1980**, *22*, 2263.

(20) (a) van Eldik, R., Ed. *Inorganic High Pressure Chemistry Kinetics and Mechanisms*; Elsevier: Amsterdam, 1986. (b) Merbach, A. E.; Akitt, J. W. In *High Pressure NMR*; Jonas, J., Ed.; Springer: Berlin, 1991; p 189.

(21) (a) Fuoss, R. M. *J. Am. Chem. Soc.* **1958**, *80*, 5059. (b) Sutin, N. *Annu. Rev. Phys. Chem.* **1966**, *17*, 119.

(22) (a) Banyai, I.; Glaser, J. *J. Am. Chem. Soc.* **1989**, *111*, 3186. (b) Banyai, I.; Glaser, J. *J. Am. Chem. Soc.* **1990**, *112*, 4703.

(23) (a) Haim, A. *Comments Inorg. Chem.* **1985**, *4*, 113. (b) Page, M. T.; Jencks, W. P. *Proc. Natl. Acad. Sci. U.S.A.* **1971**, *68*, 1678. (c) Page, M. T. *Chem. Soc. Rev.* **1973**, *2*, 295.

(24) (a) Marcus, R. A. *J. Chem. Phys.* **1965**, *43*, 1261. (b) *Annu. Rev. Phys. Chem.* **1964**, *15*, 155.

(25) (a) Dogonadze, R. R.; Kuznetsov, A. M.; Marsagishvili, T. A. *Electrochim. Acta* **1980**, *25*, 1. (b) Ulstrup, J. *Charge Transfer Processes in Condenced Media*; Springer: Berlin, 1979.

(26) (a) Nicholson, R. S.; Shain, I. *Anal. Chem.* **1964**, *36*, 706. (b) Polcyn, D. S.; Shain, I. *Anal. Chem.* **1966**, *38*, 370. (c) Wopsdhall, R. H.; Shain, I. *Anal. Chem.* **1967**, *39*, 1514, 1527, 1535.

(27) (a) Maliarik, M.; Glaser, J.; Tóth, I. *Inorg. Chem.* **1998**, *37*, 5452. (b) Maliarik, M.; Glaser, J.; Tóth, I.; da Silva, M. W.; Zékány, L. *Eur. J. Inorg. Chem.* **1998**, 565.

(28) (a) Gosser, D. K. In *A General CV Simulation Program (CVSIM)*; VCH: New York, 1993. (b) Maeda, Y.; Sato, K.; Ramaraj, R.; Rao, T. N.; Tryk, D. A.; Fujishima, A. *Electrochim. Acta* **1999**, *44*, 3441.

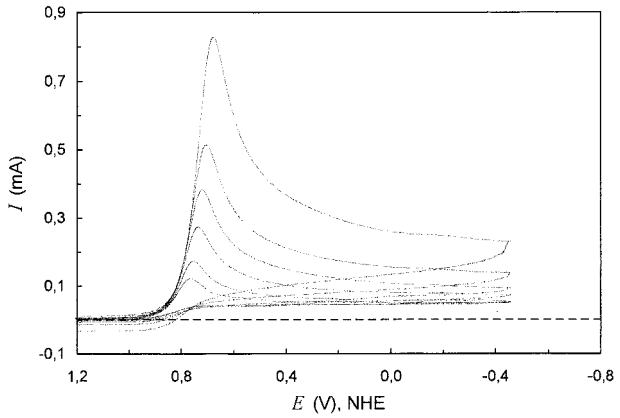

Figure 1. Cyclic voltammograms (glassy carbon electrode, area 0.1256 cm^2) for a solution containing 0.01 M $Tl(ClO_4)_3$ + 1 M $NaClO_4$ + 0.273 M $HClO_4$ at scan rates of (from top to bottom) 0.5, 0.2, 0.1, 0.05, 0.02, and 0.01 V s^{-1}, respectively.

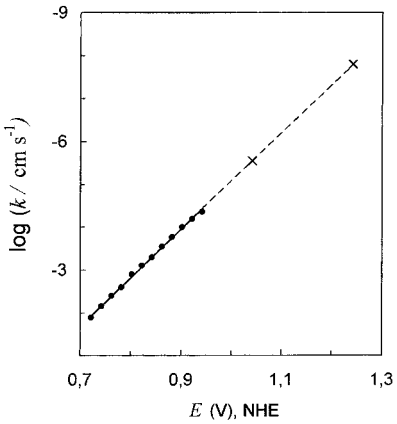

Figure 2. RDE results presented in semilogarithmic coordinates. Times signs indicate extrapolated values of log *k*, corresponding to *E*° (rejected simultaneous two-electron-transfer mechanism), and E_1* (sequential mechanism involving the dithallium intermediate, see the text for details).

was present in the solution as an internal standard (for details, see ref 32).

In Figure 1, typical voltammograms for a solution containing 0.01 M $Tl^{III}(ClO_4)_3$ + 0.0001 M $Tl^{I}ClO_4$ + 1 M $NaClO_4$ + 0.273 M $HClO_4$ obtained at different scan rates, υ, are presented. The dependence of the logarithm of the rate constant, *k*, for the reduction of Tl(aq)$^{3+}$ on the electrode potential, *E*, obtained from steady-state measurements at the RDE is presented in Figure 2. Seemingly, the reduction wave for Tl(aq)$^{3+}$ has no anodic counterpart; the peak current, I_p, is proportional to the concentration of Tl^{3+} and independent of the content of Tl^{+}. The peak potential varies with the sweep rate, shifting to less positive potentials with an increase of υ (Figure 1). The peak current is proportional to the square root of the scan rate, and the plot of the latter dependence intercepts the origin. All these properties are indicative of

(29) Bard, A. J.; Faulkner, L. R. *Electrochemical Methods. Fundamentals and Application*; Wiley: New York, 1980; Chapter 6.
(30) Greef, R.; Peat, R.; Peter, L. M.; Pletcher, D.; Robinson, J. *Instrumental Methods in Electrochemistry. Southhampton Electrochemistry Group*; Horwood: New York, 1986; Chapter 6.
(31) Bockris, J. O'M.; Reddy, A. K. N. *Modern Electrochemistry*; Plenum: New York, 1970; Vol. 2.
(32) Dolidze, T. D.; Khoshtariya, D. E.; Glaser, J.; Lindbergh, G.; Behm, M. Manuscript in preparation.

Table 1. (a) Experimental Data for the 2 equiv Reduction of Tl(aq)$^{3+}$ to Tl(aq)$^{+}$ Obtained by Cyclic Voltammetry and Rotating Disk Electrode Techniques and (b) Computer Simulation Results (for the CV Curves)

(a) Experimental Data

technique	a	$D \times 10^6$, cm^2 s^{-1}	k_2°, cm s^{-1}	E_1°, V
CV	0.66 ± 0.04	3.72 ± 0.32	(4 ± 1) × 10^{-6}	1.04 ± 0.10
RDE	0.65 ± 0.01	3.52 ± 0.10	3 × 10^{-6}	(1.04)

(b) Simulation Results

E_1°, V	E_2°, V	k_1°, cm s^{-1}	$k02$°, cm s^{-1}	α_1	α_2
1.04 (0.94−1.14)	1.46[a]	2 × 10^{-6} (10^{-5} to 10^{-7})	10^{-5} to 10^{-7}	0.65	0.4−0.5

[a] Estimated using the equation $E° = (E_1° + E_2°)/2 = 1.25$ V.[7]

an irreversible (in the electrochemical sense) charge-transfer process, which is not complicated by accompanying chemical reactions.[26a,30,31] Viz., the calculated values of the well-established criteria[26a]

$$\left(\frac{\Delta \log I_p}{\Delta \log \upsilon}\right)_{t,c} = 0.5 \tag{9}$$

and

$$\frac{\Delta E_{p/2}}{\Delta \log \upsilon} = \text{const} \tag{10}$$

(where I_p is the peak current, υ is the CV scan rate, $E_{p/2}$ is the potential at half-height) were in good agreement with this conclusion. For irreversible charge-transfer reactions the value of the product αn_α becomes available from the difference between the peak and half-peak potentials (E_p and $E_{p/2}$), and the peak potential shift, using the following equations[26a,30] (see Table 1):

$$E_p - E_{p/2} = \frac{1.86RT}{\alpha n_\alpha F} \tag{11}$$

and

$$(E_p)_1 - (E_p)_2 = \frac{RT}{\alpha n_\alpha F} \ln\left(\frac{\upsilon_1}{\upsilon_2}\right)^{1/2} \tag{12}$$

where n_α is the number of electrons transferred in a rate-determining electrochemical process, α is the corresponding transfer coefficient (vide infra), *F* is the Faraday constant, *R* is the gas constant, and *T* is the absolute temperature. The equations allow for determination of the transfer coefficient, α, provided that the number of electrons transferred in the rate-determining step, n_α, is known.

Meanwhile, the fundamental equation[29]

$$k^{el} = k^{o} \exp\left[-\frac{\alpha n_\alpha F(E - E_x^{o})}{RT}\right] \tag{13}$$

(where $k°$ is the standard heterogeneous rate constant, k^{el} is the rate constant at potential *E*, and $E_x°$ is the standard redox potential of the actual redox couple involved in the process) also allows for the determination of the value of the product αn_α by plotting log(k^{el}) vs *E* (Figure 2; see also the discussion

below). At the same time, the total number of electrochemically transferred electrons, n, is correlated to the CV peak current through the following expression derived for electrochemically irreversible reactions:[26a,30]

$$I_p = (2.99 \times 10^5) n(\alpha n_\alpha)^{1/2} A c_o D^{1/2} v^{1/2} \qquad (14)$$

where D is the reactant's diffusion coefficient, A is the area of the working electrode, and c_o is the reactant's concentration in the bulk. For a given 2 equiv electrochemical process, three different charge-transfer mechanisms can be considered (see also the Supporting Information, Figure S1).

(1) $n = 1$, in which case necessarily $n_\alpha = 1$ and, thus, $\alpha = 0.66$ (see Table 1). This mechanism, considered in some earlier work,[13] implies that the first (slow) electrochemical step is followed by a second (fast) homogeneous (chemical) disproportionation, according to the following equations:

$$2\{[Tl^{III}]^{3+} + e^- \rightleftharpoons [Tl^{II}]^{2+}\} \text{ (slow)} \qquad (15)$$

$$2[Tl^{II}]^2 \rightleftharpoons [Tl^{III}]^{3+} + [Tl^{I}]^{+} \text{ (fast)} \qquad (16)$$

This pattern in electrochemistry is known as a mechanism with chemical regeneration of the reactant, in which case all the above-mentioned criteria for clear electrochemical behavior (expressed by eqs 10−12) are violated.[26a,30,31] Thus, our electrochemical data favor the mechanism in which the entire reaction is electrochemical, corresponding to $n = 2$ (which can be either a two- or a one-step process; see below). Besides, the diffusion coefficient calculated through eq 14 with $n = 1$ yields a rather unrealistic value of 1.44×10^{-5} cm^2 s^{-1}, whereas the value of $n = 2$ yields $(3.6 \pm 0.3) \times 10^{-6}$ cm^2 s^{-1}, which is close to the typical value of 5.3×10^{-6} cm^2 s^{-1}, obtained for a triply charged ion of similar size, Ce(aq)$^{3+}$, under comparable conditions (0.1 M $HClO_4$).[28b] Hence, this mechanism can be excluded from consideration.

(2) $n = 2$, $n_\alpha = 2$, and $\alpha = 0.33$. This mechanism implies a simultaneous two-electron transfer from the electrode in a single electrochemical step, and can be excluded on the grounds of a rigorous CV peak simulation procedure (Supporting Information, Figure S1). We note that experimental CV curves cannot be replicated by the value of $\alpha = 0.33$ at any reasonable values of the other two variables, while they can be perfectly reproduced by the value of $\alpha = 0.66$ combined with reasonable values of $k°$ and $E°$ (see Figure S1, Table 1, and further discussion below; also ref 32 provides more details).

(3) $n = 2$, $n_\alpha = 1$, and $\alpha = 0.66$. This mechanism implies a sequential two-electron transfer from the electrode, provided that the transfer of the first electron is a slow (rate-determining) step, since the Tl^{2+} ion (whatever set of redox potentials is chosen; see below) is a stronger oxidant than Tl^{3+}. In such a case, when $\Delta E = E_2° - E_1° \geq 180$ mV, the shape of the combined CV waves is determined by the first electron transfer in the sequence.[26,30,31] Hence, the peak position along the potential axes should be mostly set by the standard potential $E_1°$ and the kinetic parameters $k°$ and α of the first charge-transfer step. This is in general agreement with the conclusions of earlier papers emphasizing that the transfer of the first electron (leading to the formation of Tl^{2+}) is the rate-determining step in the overall two-electron-transfer process.[7,13,14] Meanwhile, the second step is not independent and should occur immediately after the first step, but only in the potential range lower than $E_1°$. *Thus, the observation of a cathodic wave for the electrochemical reduction of Tl^{3+} at ca. 0.8 V is in contradiction with the value of $E_1° = 0.33$ V established for a one-electron reduction of $Tl^{III}(aq)^{3+}$ to $Tl^{II}(aq)^{2+}$.*[4,6] The numerical value of $E_1°$, as visible from the CV curves, should be situated between $E° = 1.25$ V and the potential where the cathodic wave rises (ca. 0.9 V), i.e., at 1.0 ± 0.1 V.

According to the theory of multistep charge-transfer processes,[31] the rate of the slow step determining the overall current is proportional to its own overpotential ($\eta = E - E_1°$). The standard rate constant was evaluated from the experimental CV curves using the fundamental equation[26a,30,31]

$$k^o = \frac{4.405 I_p}{nFAc_o \exp[(-\alpha n_\alpha F/RT)(E_1° - E_p)]} \qquad (17)$$

in which the standard potential was set equal to our value of E_1. The obtained value, $k° = (4 \pm 1) \times 10^{-6}$ cm s^{-1}, is in good agreement with the one calculated from the steady-state log k vs E relationship using the same value for $E_1°$ (see Figure 2). The computer simulation procedure also revealed that with the experimentally determined values of $\alpha = 0.66$ and the diffusion coefficient of 3.68×10^{-6} cm^2 s^{-1} (Table 1) at any reasonable values of $k°$, *the value of $E_1°$ should in no case differ from 1.04 ± 0.10 V* (in the following, the equilibrium potentials obtained in the present work are denoted as E*). Results of the simulation procedure also set the frames for the characteristic parameters for the second step; the latter was proven to be electrochemical too (cf. the Supporting Information, Figure S1, and Table 1).[29]

The present values of E_1* = 1.04 ± 0.1 V and E_2* = 1.46 ± 0.1 V (the latter estimated using the overall value) differ dramatically from the values of 0.33 ± 0.05 and 2.22 ± 0.05 V, respectively, obtained earlier for 1 equiv redox cross-reactions,[18] and/or on the basis of experiments with Tl(aq)$^{2+}$ generated directly by flash photolysis, or by pulse radiolysis of thallium(III) solutions.[6] Obviously, the equilibrium potential E_1* showing up in our electrochemical experiment and the calculated value of E_2* are not the properties of the "free" aqueous divalent thallium ion, Tl(aq)$^{2+}$, but rather they characterize divalent thallium in some other intermediate state. Our values almost coincide with the values estimated earlier by Hush on the basis of a two-step model (1.0 and 1.5 V, respectively).[10] This suggests involvement of similar intermediate states in both the homogeneous and electrochemical processes. Acceptance of values for the standard reduction potentials estimated by Hush automatically leads to the free energy gap of the intermediate state 30−35 kcal mol^{-1} lower compared to the above-discussed value of 43 kcal mol^{-1}, i.e., ∼10 kcal mol^{-1}. The latter value is fully compatible with the experimental activation free energy of the process (see ref 10b and the Discussion). Apparently,

the difference of 30−35 kcal mol^{-1} is in agreement with the energy of covalent 6s−6s bonding established for dimers isoelectronic to the $Tl^{II}-Tl^{II}$ moiety.[16a,b] Some 6s−6p_z overlap is also possible and may contribute to the bond stability since the Au−Au and Hg−Hg bonds appear to be more stable than that of, e.g., Cs−Cs in Cs_2, where the bonding is limited to 6s overlap. Ab initio calculations for the Hg−Hg bonding gave a value of ca. 70 kcal mol^{-1},[16b] without taking into account the electrostatic repulsion between ions. For the $Tl^{2+}-Tl^{2+}$ moiety, with its much larger repulsion energy and crystallographic thallium−thallium distance of about 2.9 Å,[15] a total internuclear bonding energy of 30−40 kcal mol^{-1} can be estimated. In our model calculations a thallium−thallium bonding energy of 34 kcal mol^{-1} is used (see below).

The possible formation of a strongly adsorbed Tl^{2+} (on glassy carbon) as an intermediate can be excluded considering the perfect character of I_p vs $v^{1/2}$ plots. Also, the appearance of additional prepeaks is expected in such a case;[26c,30] however, they never appear in the experiments. Hence, after Taube,[4b] taking into account Hush's[10] estimate for the reduction potentials for the two-step mechanism (vide infra) and the above-discussed structural data,[15,16] we propose that the transient complex exhibiting the unusual reduction potential is a directly metal−metal bonded intermediate, $[(aq)Tl^{II}-Tl^{II}(aq)]^{4+}$. This is an inner-sphere two-electron-transfer mechanism which probably takes place also for some other well-known cross-exchange processes, such as $Tl^{3+} + Hg^0 \rightleftharpoons [Tl^{II}-Hg^{I}]^{3+} \rightleftharpoons Tl^{+} + Hg^{2+}$, forming an individual reaction type.[18b] In another class of inner-sphere 2 equiv processes metastable binuclear intermediates, e.g., $[Pt^{III}-Tl^{II}]$, detectable by different spectroscopic techniques, can be formed.[27] These peculiarities, along with internuclear electrostatic interactions and ligand effects, can be explained by the effect of inert electron pairs characteristic of s-type valence electrons.[4c] This effect is partially eliminated for the latter system due to the participation of 5d electrons of Pt (see also the Discussion, part c).[27] In contrast, the homogeneous 1 equiv cross-reactions involving Tl^{3+}, or Tl^{+}, including one-electron exchange processes

$$Tl^{3+} + Tl^{2+} \leftrightarrows Tl^{2+} + Tl^{3+} \quad (18)$$

$$Tl^{2+} + Tl^{+} \leftrightarrows Tl^{+} + Tl^{2+} \quad (19)$$

obviously take place via the simple outer-sphere mechanism, in which these ions exhibit their normal redox potentials, eqs 3 and 4, and constitute a different reaction type which exhibits a curved free energy relationship.[18] Direct comparison of these reaction types at $\Delta G_o = 0$ reveals a ratio of the activation free energies of 2, whereas if the two-electron process is also outer-sphere (a case of the closely resembling one- and two-electron-transfer mechanisms), a ratio of 4 could be expected on the basis of Marcus theory (see the next section for details).

Discussion

The relevant theoretical basis for the discrimination of different microscopic charge-transfer mechanisms is the Marcus-type expression for the activation free energy, which in this particular case can be expressed as[1a,24,25]

$$\Delta G_a = W_i + \Delta G^{\ddagger} = W_i + \Delta G_i + \frac{(\Delta G_o + \Delta G_r - \Delta G_i + \Delta G_f - W_i + W_f)^2}{4\Delta G_r} - H_{if} \quad (20)$$

Here ΔG_a is the experimental activation free energy, W_i is the equilibrium free energy (work term) of the precursor complex formation, W_f is the equilibrium free energy (work term) of the complex formation by the reaction products (with almost intact solvating shells), $\Delta G^{\ddagger}$ is the intrinsic activation free energy of the rate-determining elementary charge-transfer step (either one-electron or two-electron, outer- or inner-sphere, vide infra), ΔG_i is the free energy of bringing the reactant ions from the precursor state to the transition state of covalent bond formation, accordingly, ΔG_f is the free energy of bringing the product ions from the successor state to the transition state (implying the inner-sphere superexchange mechanism of simultaneous two-electron transfer; see below), ΔG_o is the free energy gap of the (rate-determining) intrinsic charge-transfer step, and ΔG_r is the reorganization free energy of that step including the terms due to the reorganization of the first solvation shell, ΔG_{is}, and the rest of the solvent, ΔG_{os} ($\Delta G_r = \Delta G_{is} + \Delta G_{os}$). It should be noted here that the terms ΔG_i and ΔG_f are absent in the cases of outer-sphere mechanisms (one- or two-electron), and the terms W_i and W_f and ΔG_i and ΔG_f entering the quadratic term of eq 20 cancel for the cases of symmetric intrinsic self-exchange (for both the inner-sphere and outer-sphere mechanisms, vide infra).[24,25]

Application of eq 20 implies that the contribution to the experimental activation free energy arising from the inter-reactant interaction, i.e., the value of the free energy required for bringing these ions into close contact (at a distance close to the energy minimum position of the proposed $Tl^{II}-Tl^{II}$ covalent bond, ca. 2.9−3.1 Å), can be divided into two terms, W_i and ΔG_i. The first term is associated with the equilibrium free energy of formation of the precursor complex, with almost intact solvating shells. This free energy (work) term is usually expressed through the simple Coulomb[2b,10] or more advanced Bjerrum−Fuoss[21,22] equations, but in fact it can be almost entirely identified as a negative entropy associated with an increase of solvation (attending the charge concentration),[23a] and a loss of translational and rotational degrees of freedom upon the precursor formation.[23b,c] The corresponding experimental and calculated values of W_i, for the encounter of 3+/1+-charged aqua and related complexes, vary between 4 and 6 kcal mol^{-1}.[10,22]

The second term, ΔG_i, which in contrast to the preequilibrium term essentially belongs to the intrinsic kinetic (charge-transfer) step, is determined by a closer approach of reactant ions until the transition state along this particular reaction coordinate is derived (see the discussion below), which is close to the configuration of a covalently interacting but still extremely unstable (virtual) state characterized by a Tl−Tl separation of 2.9 Å. The latter motion requires an

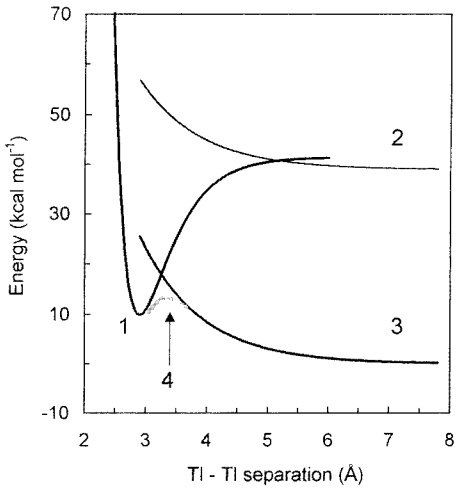

Figure 3. Arrangement of the free energy terms reflecting the motion of a reacting Tl−Tl system along the metal−metal separation coordinate: (1) $Tl^{II}-Tl^{II}$ attractive branch; (2) $Tl^{II}-Tl^{II}$ repulsive branch; (3) $Tl^{III}-Tl^{I}$ repulsive branch; (4) the curve indicating the adiabatic (actual) free energy profile for a homogeneous superexchange process (for channel terms 1 and 2 the adiabatic splitting is not shown for clarity; see the text).

essential deformation of the solvation shells and can be compared to the process of water exchange in the first solvation sphere of the $Tl(aq)^{3+}$ ion (the latter is less labile than that of the $Tl(aq)^{+}$ ion) and the overall associative mechanism. The value of the corresponding activation free energy, after subtraction of the previously considered encounter contribution, can be deduced to be on the order of 5−6 kcal mol^{-1}, or so ($k_{ex} \approx 5 \times 10^8$ to 5×10^9 s^{-1}.[4b,22b] In total, the sum of these quantities, ca. 11 kcal mol^{-1}, can be estimated as a contribution of nonsolvent factors to the overall free energy of activation.[1a,24,25]

(i) Microscopic Mechanism for Homogeneous Self-Exchange. Recently, a three-state model for outer-sphere two-electron-transfer reactions was developed,[2] while the outer-sphere superexchange mechanism involving a virtual intermediate state was also reconsidered.[17a] Extension of these models allows for the analysis of microscopic mechanisms through the inner-sphere pathways, proposed above for the present case.[17b] For this purpose, in addition to the generalized solvent reorganization coordinate, we consider below also the motion along the thallium−thallium separation coordinate, which, according to arguments discussed above, should play a key role in the microscopic mechanism.

Figure 3 represents the free energy change for the Tl−Tl system as a function of the metal−metal separation distance. The repulsive and attractive terms (the latter mostly covalent in origin) are shown schematically, and the possible local minima for the precursor states Tl^{3+}/Tl^{+} and Tl^{2+}/Tl^{2+} are not indicated in the corresponding repulsive terms. The resonance splitting of intercepting channel (diabatic) terms (the lower adiabatic free energy profile) is depicted for channel terms 1 and 3 only for clarity, and indicated by an arrow (fragment 4, Figure 3). The lower terms are drawn to result in a free energy gap of ca. 11 kcal mol^{-1} for the intermediate state (vide infra). For the present system, as far as the covalent interaction between the two metal centers is involved, the motion along the internuclear separation coordinate should be preferred, so that the medium (outer-shell) reorganization energy scales with the square of the net charge to be transferred in the elementary step:[1a,24,25,33]

$$\Delta G_{os} = (\Delta e)^2\left(\frac{1}{\epsilon_o} - \frac{1}{\epsilon_s}\right) f(R, a_i) \qquad (21)$$

Here, Δe is the net charge transferred in the elementary step, ϵ_o and ϵ_s are the optical and static dielectric constants of the solution, respectively, and $f(R, a_i)$ is a function of the interreactant charge-transfer distance, R, and other geometric characteristics of the reactive system, such as, e.g., the effective radii of the reactants, a_i, or similar characteristics, depending on the theoretical model applied. For the case of $R \geq a_1 + a_2$, this function has a simple form derived by Marcus:[24,33,35,36]

$$f(R, a_i) = \frac{1}{2a_1} + \frac{1}{2a_2} - \frac{1}{R} \qquad (22)$$

Other models[36,37] consider the case of $R < a_1 + a_2$, for which more cumbersome equations were derived (see the Supporting Information, eqs S2 and S3). Application of these models is sufficient for a more realistic situation when the first solvation sphere cannot be regarded as having "bulk" properties, but rather as the ligand sphere, requiring special consideration.[35,36] For homogeneous charge transfer all the models predict an increase of ΔG_{os} with R (see the Supporting Information, Figure S2).

Let us now, on the basis of the obtained numerical data, discuss possible microscopic mechanisms for the overall two-electron self-exchange. Some of these mechanisms regarding the free energy change along the medium (solvent) reorganization coordinate are depicted in Figure 4 and the corresponding calculated free energy parameters are listed in Table 2.

(a) Sequential Transfer Involving Two "Free" $Tl(aq)^{2+}$ Ions in the Intermediate State (Involving the Energy Terms 1, 4, and 1′, Figure 4). This mechanism requires a free energy gap of 43 kcal mol^{-1} (for the first electron-transfer step). With an estimated 1 equiv minimal outer-sphere reorganization free energy of 12.5 kcal mol^{-1} (taken as 1/4 of the 2 equiv contribution at the contact ion configuration requiring $W_i + \Delta G_i = 11$ kcal mol^{-1}, Table 2), according to eq 20, one encounters a situation which is the mirror of the inverted Marcus region with $\Delta G_a^{calcd} \approx 70$ kcal mol^{-1}. We note that within this model there is no source for the lowering of ΔG_a ($\Delta G^{\ddagger}$) through very adverse (for such a mechanism) ΔG_o. The "cage effect" discussed in an earlier

(33) Krishtalik, L. I. *Charge Transfer Reactions in Electrochemical and Chemical Processes*; Plenum: New York, 1986.
(34) (a) Khoshtariya, D. E. *J. Mol. Struct.: THEOCHEM* **1992**, *255*, 131. (b) Khoshtariya, D. E.; Berdzenishvili, N. O. *Chem. Phys. Lett.* **1992**, *196*, 607.
(35) (a) Krishtalik, L. I. *Elektrokhimiya* **1982**, *18*, 1512. (b) *J. Electroanal. Chem*. **1982**, *136*, 7.
(36) (a) Dzhavakhidze, P. G.; Kornyshev, A. A.; Krishtalik, L. I. *J. Electroanal. Chem*. **1987**, *228*, 329. (b) Phelps, D. K.; Kornyshev, A. A.; Weaver, M. J. *J. Phys. Chem*. **1990**, *94*, 1454.
(37) (a) Newton, M. D. *Chem. Rev*. **1991**, *91*, 767. (b) Billing, R.; Khoshtariya, D. E. *Inorg. Chem.* **1994**, *33*, 4038. (c) Rosso, K. M.; Ruistad, J. R. *J. Phys. Chem. A* **2000**, *104*.

Table 2. Estimated Values for the Different Components of the Experimental Activation Free Energy (kcal mol^{-1}) (Eq 20)[a]

parameter/mechanism	outer-sphere sequential	outer-sphere simultaneous	inner-sphere superexchange	electrochemical sequential
ΔG_o	43	0	0	17 (0)
ΔG_o^{intr}			11	
W_i (R)	5 (8.0)	5 (8.0)	5 (8.0)	~0
ΔG_i (R)	~3 (5.2)	~3 (5.2)	6 (2.93.1)	
	~0 (8.0)	~0 (8.0)		
(I) ΔG_r (R)	35 (5.2)	140 (5.2)	64 (3.1)	~60 (34)
	48 (8.0)	190 (8.0)	51 (2.9)	(Kornyshev)
(II) ΔG_r (R), at fixed $\Delta G_{is} = 32$	20 (5.2)	80 (5.2)	53 (3.1)	24 (34)
	30 (8.0)	120 (8.0)	51 (2.9)	(Marcus)
H_{if}	0.1	0.1	~5	<1
(I) ΔG_a^{calcd} (R)	38 (5.2)	40 (5.2)	24 (3.1)	~24
	40 (8.0)	52 (8.0)	20 (2.9)	
(II) ΔG_a^{calcd} (R)	42 (5.2)	28 (5.2)	21 (3.1)	~6
	38 (8.0)	35 (8.0)	20 (2.9)	

[a] Reorganization free energies at fixed internuclear distance R (Å) are calculated according to eqs 21, 22, 30, S1, and S2.

paper,[11b] without considering a covalent interaction, leaves room only for an additional unfavorable Coulombic (repulsive) force, leading to an increase of ΔG_o and ΔG_a.

(b) Outer-Sphere Simultaneous Two-Electron Transfer (Involving the Energy Terms 1 and 1′ Only, Figure 4). This mechanism suggests an interreactant distance ($R = a_1^{eff} + a_2^{eff}$) of ca. 7−8 Å, implying almost intact inner solvation shells for both reactant ions. The corresponding reorganization free energy amounts to at least $\Delta G_r = 100$ kcal mol^{-1} and a formation free energy W_i of 5 kcal mol^{-1} for the encounter complex. According to eq 20, at $\Delta G_o = 0$ and $\Delta G_i = 0$, these values result in $\Delta G_a^{calcd} = 30$ kcal mol^{-1} (Table 2). Considering a closer approach (an intact inner shell for Tl^{3+} and labile inner shell for Tl^{+}) at 5.0−5.2 Å, one encounters the situation where ΔG_r is at least 80 kcal mol^{-1} and $W_i + \Delta G_i \approx 6-7$ kcal mol^{-1}, yielding $\Delta G_a^{calcd} \approx 26-28$ kcal mol^{-1}. This value is rather close to $\Delta G_a^{exptl} = 23.4$ kcal mol^{-1}, and can be considered as supporting the outer-sphere mechanism with partial desolvation. However, without considering the Tl−Tl covalent interaction, for the outer-sphere two-electron-exchange matrix element, the following equation can be applied:[17b]

$$H_{13} \approx \frac{H_{12}H_{23}}{|\Delta G_o - \Delta G_{os}{}^{31}|} \qquad (23)$$

where H_{12} and H_{23} are outer-sphere electronic coupling matrix elements. For simple outer-sphere one-electron-transfer processes involving aqua and comparable complexes of metal ions, it is has been established that $H_{if} \leq 0.5\ k_B T$.[37] Hence, for this model, $H_{13} \leq 0.1$ kcal mol^{-1}, corresponding to the nonadiabatic regime with an unfavorable preexponential factor (transmission coefficient <1). *Thus, we note that implementation of a close approach of the reactant ions (~2.9 Å), implying a deformation of both inner shells and favoring Tl−Tl covalent interaction, automatically leads to another mechanism for the simultaneous two-electron transfer, viz., to the inner-sphere mechanism, via the virtual intermediate state* (see the further discussion below).

(c) Sequential Transfer Involving the Metastable $[Tl^{II}-Tl^{II}]^{4+}$ Intermediate (Not Shown in Figure 4). This inner-sphere mechanism implies a two-step two-electron transfer involving an energetically relaxed (thermodynamically stable) dinuclear intermediate. The free energies corresponding to such a mechanism formally should be $\Delta G_o < 0$, and/or $\Delta G_f \gg \Delta G_i$. This was observed for processes of the type[38] $Pt^{IV} + Tl^{III} \rightleftharpoons [Pt^{III}-Tl^{II}] \rightleftharpoons Pt^{II} + Tl^{I}$ where the covalently bonded intermediate (thermodynamically metastable) is stabilized kinetically so that it can be isolated and characterized as individual species.[27] In the present case, the intermediate $[Tl^{II}-Tl^{II}]^{4+}$ formed through the homogeneous process is essentially unstable, both thermodynamically and kinetically, and thus can be considered as a virtual intermediate only (see the next subsection).

(d) Simultaneous Two-Electron Transfer via the Virtual Intermediate (Superexchange Mechanism, Involving the Energy Terms 2, 3, and 2′, Figure 4). Such a mechanism[17b] is possible for the present system due to the thermodynamically and kinetically unstable character of the proposed intermediate, $[Tl^{II}-Tl^{II}]^{4+}$. According to the extended version of charge-transfer theory in three-state redox systems, for the overall two-electron matrix element operating through the superexchange mechanism, the following expression can be applied:[17b]

$$H_{13} = \frac{H_{12}H_{23}}{|\Delta G_o{}^{21} - (\Delta G_o{}^{31}/2) - (\Delta G_{os}{}^{31}/2)|} \qquad (24)$$

where H_{12} and H_{23} are the one-electron-transfer matrix elements, $\Delta G_o{}^{21}$ and $\Delta G_o{}^{31}$ are the free energy gaps for the first one-electron-transfer process and the overall two-electron-transfer process, respectively, and $\Delta G_{os}{}^{31}$ is the solvent reorganization free energy for the simultaneous two-electron transfer within the same system. The superexchange mechanism through the $[Tl^{II-}Tl^{II}]^{4+}$ intermediate implies combination of two two-electron inner-sphere processes of the covalent-to-ionic and reverse transition types. For simple one-electron transitions of this type, $H_{if} \approx 10$ kcal mol^{-1}. Estimates obtained above suggest that the free energy gap for the $[Tl^{II}-Tl^{II}]^{4+}$ formation (ca. 11 kcal mol^{-1}) almost coincides with the value of $W_i + \Delta G_i$ estimated for the inner-sphere mechanism. This leads to $\Delta G_o{}^{21} \approx 0$, and $\Delta G_o = \Delta G_o{}^{31} = 0$. This also means that for a homogeneous self-exchange process the transition state along the Tl−Tl

separation coordinate coincides with, or is very close to, the final ("equilibrium") state corresponding to the maximal covalent stabilization (Figure 3). The maximum on the resulting adiabatic surface is not expected to be well-pronounced because of a large resonance splitting of the energy terms amounting to $2H_{12} = 2H_{23} \approx 20$ kcal mol^{-1}, or so. The transition-state Tl−Tl separation distance (nearly the equilibrium distance for covalent bonding) of 3.2−3.4 Å suggests a 2 equiv solvent reorganization free energy of ca. 60 kcal mol^{-1} (Figure S2). This value, together with $\Delta G_o = 0$, ΔG_o[21] $\approx W_i + \Delta G_i = 11$ kcal mol^{-1}, and $H_{13} \approx 5$ kcal mol^{-1} (estimated by means of eq 24), yields $\Delta G_a^{calcd} \approx$ 22−24 kcal mol^{-1}, and a transmission coefficient close to unity, in good agreement with published experimental data.[5a,10]

Summarizing the situation for the homogeneous two-electron self-exchange, we conclude that the superexchange mechanism through the virtual, yet covalently interacting, $[Tl^{II}-Tl^{II}]^{4+}$ state seems most probable from the viewpoint of both factors determining the rate constant, free energy of activation, and electronic coupling. In this context it can be noted that also the simultaneous two-electron transfer (dislocation) in the processes of this type should be considered as "correlated" rather than "parallel" because at the close approach of the reactant ions, the two electrons experiencing the exchange interaction cannot be considered as fully equivalent. In other words, it is not necessary for two electrons of the "donor" $Tl(aq)^+$ ion, situated on the 6s atomic orbital, to be transferred in parallel. Instead, at some moment upon the approach of the two ions the frontier electron can gradually change its "affiliation" from the AO to the MO type, while another one instantaneously located in the space-separated position may undergo a through-space hopping. Such an asymmetry between two "mobile" electrons will increase as the overall mechanism gradually changes from outer-sphere to inner-sphere. We also note that the validity of eq 24 is restricted to the cases when the intermediate state is essentially virtual (that is, undetectable by conventional techniques as an individual species).[17b] Otherwise, each step of the formation and breakdown of the intermediate should be considered as separate chemical processes.

(ii) Microscopic Mechanism for an Electrode Process. For the electrode reduction of $Tl(aq)^{3+}$ to $Tl(aq)^+$ on the basis of the present and literature data, we assume that the intermediate state, namely, the covalently bonded $[Tl^{II}-Tl^{II}]^{4+}$ ion, is formed with a formal reduction potential of $E_1^* = 1.04$ V, leading to the reduction potential of the next step, $E_2^* = 1.46$ V. But, in contrast to the homogeneous self-exchange process, the formation of the $Tl(aq)^{2+}$ ion as a thermodynamically metastable particle is unavoidable. Thus, for the mechanism of the transfer of the first electron, one can write

$$Tl^{III}(aq)^{3+} + e^- \rightleftharpoons Tl^{II}(aq)^{2+} \text{ (slow)} \qquad (25)$$

$$2Tl^{II}(aq)^{2+} \rightleftharpoons [Tl^{II}-Tl^{II}]^{4+} \text{ (fast)} \qquad (26)$$

The situation here is somewhat analogous to the cathodic hydrogen evolution reaction, where the hydrogen atom formed in a first rate-determining step waits for another one to form molecular hydrogen in a fast activationless process.[33] The difference is that, in the case of hydrogen evolution, the intermediate particle (hydrogen atom) is adsorbed on the Pt electrode (which is clearly manifested in the corresponding CV curves; see, e.g., ref 30, Figure 6. 22), whereas the step of dithallium ion formation (eq 26) probably takes place at some distance from the electrode surface, presumably at the OHP (outer Helmholtz plane,[3a] as follows from the analysis of our CV curves). Results of the model calculations by Koper and Schmickler[3a] support the latter conclusion. They indicate that strongly solvated and, thus, effectively large ions such as, e.g., $Tl(aq)^{3+}$, prefer to exchange electrons with the electrode from a larger distance, in contrast to easily desolvated univalent ions which prefer to react through the step of "ion transfer", leading to a specific adsorption of reactant ions (see also the discussion below). The Nernst equation for this chemical system, operating through eqs 25 and 26, thus reads

$$E_1^* = E_1^{\circ *} + \frac{RT}{F} \ln\left(\frac{[Tl^{3+}]}{[Tl_2^{4+}]^{1/2}}\right) \qquad (27)$$

where $E_1^{\circ *}$ is the formal redox potential and E_1^* is the standard redox potential of the $Tl^{3+}/(^1/_2[Tl_2]^{4+})$ couple. This is because the dimerization of two $Tl(aq)^{2+}$ ions in this particular case is an activationless process (involving the channel terms 2 and 1, Figure 3), and its rate is limited only by the frequency factor of the encounter complex formation multiplied by the "waiting" factor for another $Tl(aq)^{2+}$ formation during the lifetime of the first $Tl(aq)^{2+}$ ion (both are proposed to be formed within the area of the OHP). Still, the latter process seems more probable compared to the direct reduction of the $Tl(aq)^{2+}$ ion, which requires a little activation (see below). Seemingly, a little activation is also required by the reverse process of the oxidation of $Tl(aq)^{2+}$ to $Tl(aq)^{3+}$, which is competitive with the dimerization process but less probable (see below). Unlikely for the value of E_1^* (operating in eqs 25 and 26), the transfer coefficient of the first step, α_1, should be determined by the relative position of "solvent" free energy terms of states $Tl(aq)^{3+}$ and $Tl(aq)^{2+}$ (i.e., solely by eq 25; see, e.g., ref 33). The relative position of the free energy terms for the electrode process under consideration at the electrode potential $E = E_1^* = 1.04$ V is depicted in Figure 5. The energy levels of all states are shown with respect to a generalized solvent reorganization coordinate. This figure is complementary to Figure 3 (upper curve) representing the free energy change along the Tl−Tl separation coordinate.

According to the general theory[1a,24,25,33]

$$\alpha = \frac{1}{2} + \frac{\Delta G_o}{2\Delta G_r} \qquad (28)$$

Implying that the experimental value, $\Delta G_o = {}^1/_2(\Delta H_{Tl-Tl}) \approx 17$ kcal mol^{-1}, correctly reflects the microscopic mechanism, our experimental value of $\alpha_1 = 0.65$ suggests that

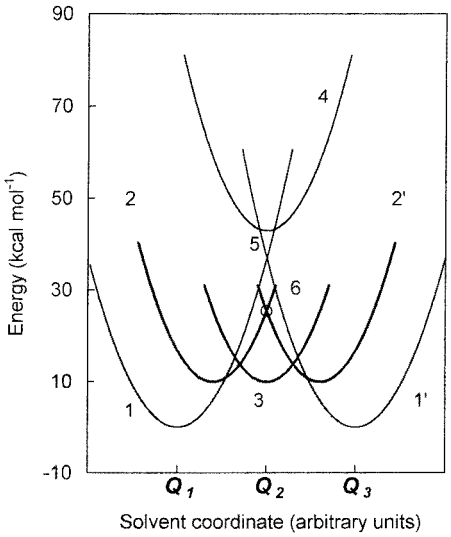

Figure 4. Arrangement of the homogeneous two-electron-transfer (self-exchange) free energy terms along the medium (solvent) reorganization coordinate: (1) initial state; (1′) final state; (2 and 2′) "initial" and "final" states along this coordinate, corresponding to a region of the transition state ($R \approx 3.2-3.4$ Å) along the Tl−Tl separation coordinate (Figure 3); (3) virtual intermediate state corresponding to the Tl−Tl covalent distance, $R = 2.9$ Å (Figure 3); (4) a hypothetical (unrealistic) intermediate state involving "free" $[Tl^{II}]^{2+}$ ions; (5) a hypothetical transition state for the outer-sphere (parallel) two-electron-transfer process; (6) a hypothetical transition state for the "inner-sphere" two-electron process in the absence of a virtual intermediate state (indicated by a circle). The inner-sphere superexchange mechanism is realized through two lower intersections of the bold parabolas.

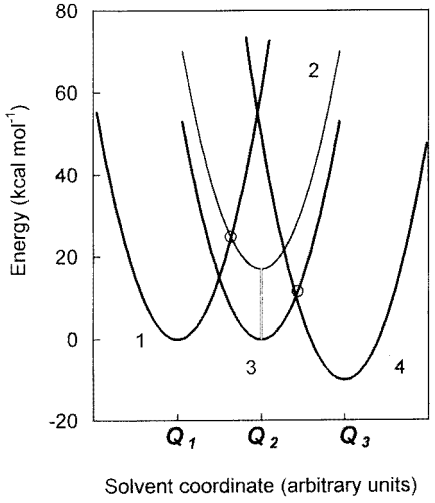

Figure 5. Arrangement of the electrode two-electron-transfer (reduction of $Tl(aq)^{3+}$ to $Tl(aq)^{+}$) free energy terms along the medium (solvent) reorganization coordinate: (1) the initial $Tl(aq)^{3+}$ state; (2) the intermediate $Tl(aq)^{2+}$ (transition) state; (3) the $^1/_2[Tl^{II}-Tl^{II}]^{4+}$ intermediate (thermodynamically disclosed) state; (4) the final $Tl(aq)^{+}$ state. Two intermediate states (3 and 4) correspond to different positions along the Tl−Tl separation coordinate, R (curves 2 and 1, respectively, Figure 3). Transition states are indicated by circles.

$\Delta G_r \approx 60$ kcal mol^{-1}.[38] Koper and Schmickler[3a] theoretically estimated the same value for the solvent reorganization free energy for the electrode process

$$Zn(aq)^{2+} + e^- \rightleftharpoons Zn(aq)^{+} \quad (29)$$

occurring via a through-space electron-transfer pattern. The Marcus equation for the solvent reorganization free energy of the electrode process[24,33,35,36]

$$f(R, a) = \frac{1}{2a} - \frac{1}{4R} \quad (30)$$

for the realistic effective radius of the reactant ion, $a_h = 2.6$ Å, and the charge-transfer distance of 3−4 Å yields a value of $\Delta G_r^{el} \approx 25-30$ kcal mol^{-1}. The qualitatively different trend of the dependence of ΔG_r^{el} on R, and much larger values of ΔG_r^{el} for these kinds of electrochemical steps, can be predicted on the basis of the model of Kornyshev et al.,[36] taking into account nonlocal electrostatic effects of field penetration into the electrode and the solvent mode spatial dispersion (see also the Supporting Information, Figure S3). Table 2 illustrates the results of calculations based on Marcus' and Kornyshev's models.

According to the present microscopic model, the transfer of the second electron should take place to the dithallium complex $[Tl^{II}-Tl^{II}]^{4+}$, a process with a free energy gap ΔG_o[22] of ~ -10 kcal mol^{-1}. This suggests a value of $\alpha_2 \approx 0.4-0.5$ (if one accepts the same value of the solvent reorganization free energy as was proposed for the first electron-transfer step). The latter value of α_2 is compatible with the results of the computer simulation procedure for the resulting CV curve (Table 1).

It is interesting to note that the reverse two-electron-transfer process, namely, the oxidation of $Tl(aq)^{+}$ to $Tl(aq)^{3+}$, is expected to exhibit an anodic wave near $E = E_2^* = 1.46$ V, upon reverse potential scanning. According to the principle of microscopic reversibility, the situation with the free energy terms at $E = 1.46$ V should be similar to that shown in Figure 5 (changed symmetrically with respect to the Tl^{3+} and Tl^{+} terms). The logical microscopic mechanism should include the following paths for the first electron-transfer step:

$$Tl(aq)^{+} - e^- \rightleftharpoons Tl(aq)^{2+} \text{ (slow)} \quad (31)$$

$$2Tl(aq)^{2+} \rightleftharpoons [Tl^{II}-Tl^{II}]^{4+} \text{ (fast)} \quad (32)$$

In fact, no anodic wave due to this process was detected under our experimental conditions, within the potential range of 1.0−2.0 V (cf. the Experimental Section). Instead, hysteresis-type irregular current/voltage curves were observed above $E = 1.5$ V, probably due to oxygen evolution and formation of oxide films on the electrode surface (see, e.g., refs 29 and 30). Obviously, some mechanism is blocking the oxidation process of $Tl(aq)^{+}$, which can be microscopically reversed to that considered above (eqs 25 and 26). The most probable reason for such a "disorder" may originate from essentially different solvating features of the $Tl(aq)^{3+}$ and $Tl(aq)^{+}$ ions as the starting reactants. As already mentioned above, according to Koper and Schmickler[3a] for highly charged and effectively large aqua-coordinated ions such as $Tl(aq)^{3+}$, the most probable redox path is through-space electron hopping to/from the OHP. Meanwhile, for

(38) The estimate is based on the assumption that within the considered potential range $\alpha = \text{const}$. This assumption is quite common for traditional electrochemistry, but is strictly valid for cases where $\Delta G_o \ll \Delta G_r$.[24,25,33] We assume that this roughly holds in the present case, validating also the application of eq 13.

easily desolvable univalent ions such as $Tl(aq)^+$, a more probable redox path implies ion transfer to the electrode followed by a strong specific adsorption on the electrode surface as the rate-determining step:

$$Tl(aq)^+ + \delta e^- \rightleftharpoons Tl_{ads}^{(1-\delta)+} \text{ (slow)} \quad (33)$$

$$Tl_{ads}^{(1-\delta)+} + (1-\delta)e^- \rightleftharpoons Tl_{ads}^{2+} \text{ (fast)} \quad (34)$$

In this case, Tl_{ads}^{2+}, formed as an intermediate, is probably trapped in a local potential minimum at the electrode surface, at least during the time interval sufficient to prevent the dimerization process (making it less favorable compared to the competing process of the second electron transfer from the adsorbed state). Thus, the formal reduction potential for the corresponding first electrochemical step will be close to the formal reduction potential of the process given by eq 4, which falls far above the region available for the reliable electrochemical measurements on a glassy carbon electrode.

Conclusions

Electrochemical data obtained in the present work strongly suggest that in the course of 2 equiv reduction of $[Tl^{III}]^{3+}$ to $[Tl^{I}]^{+}$ at the electrode thermodynamically and kinetically active intermediate species, different from $[Tl^{II}]^{2+}$, are formed with a formal redox potential of $E_1^* = 1.04$ V. Analysis of CV curves indicates that in the cathodic process the intermediate ion cannot be an adsorbed divalent thallium, but rather is a covalently bonded dithallium complex, $[Tl^{II}-Tl^{II}]^{4+}$, formed near the electrode, probably at the OHP.

In the case of the homogeneous two-electron self-exchange between $Tl^{III}(aq)^{3+}$ and $Tl^{I}(aq)^{+}$, formation of such an intermediate is experimentally undetectable at present, but seems to be unavoidable through the most probable inner-sphere mechanism. The outer-sphere simultaneous (parallel) and sequential single-electron-transfer mechanisms can be excluded on the grounds of kinetic and thermodynamic arguments, respectively. Hence, the work terms of bringing the reactant ions at the distance of $Tl^{II}-Tl^{II}$ covalent interaction largely contribute to the activation free energy of a homogeneous self-exchange process, while the contribution of the medium reorganization free energy is lowered about 4 times compared to that of the alternative outer-sphere simultaneous two-electron-transfer mechanism.

In contrast, in the course of an electrochemical process of a two-electron reduction of $[Tl^{III}]^{3+}$, the $[Tl^{II}-Tl^{II}]^{4+}$ complex, seemingly showing up in the reduction potential, can be formed without appreciable thermal activation immediately after the electrochemical transfer of electrons to $[Tl^{III}]^{3+}$ and formation of two neighboring $Tl^{II}(aq)^{2+}$ ions, which, before the transformation into the $[Tl^{II}-Tl^{II}]^{4+}$, in fact, exists in the transition state only. The activation free energy of the slow electrochemical step mostly originates from the medium reorganization. However, in the 2 equiv electrochemical process of $[Tl^{I}]^{+}$ oxidation the mechanism is not microscopically reversible, due to the operation of an alternative ion-transfer mechanism.

Acknowledgment. This work was made possible thanks to the continuous support from the Swedish Natural Sciences Research Council (NFR) and from the European Commission through INTAS Project No. 96-1162. D.E.Kh. and L.D.Z. also kindly acknowledge Collaborative Linkage Grant PST.CLG 975701 from the North Atlantic Treaty Organization. We are indebted to Mr. M. Behm for expert assistance in the experimental work and to Drs. N. Hush, D. N. Beratan, W. Schmickler, I. Tòth, and M. Maliarik for helpful comments.

Supporting Information Available: Discussion of solvent reorganization free energy and figures showing cyclic voltammograms for a scan rate of 0.1 V s^{-1} and simulated CV curves for three sets of parameters, the calculated dependence of the homogeneous two-electron-transfer solvent reorganization energy on the metal−metal separation distance, and the calculated dependence of the electrochemical one-electron solvent reorganization free energy on the electrode−reactant separation distance. This material is available free of charge via the Internet at http://pubs.acs.org.

IC0100525